4th Intercontinental Geoinformation Days

igd.mersin.edu.tr

Introducing a new approach to temperature validation of remote sensing thermal images

Hassan Emami *[1], **Arash Rahmanizadeh** [1]

[1]University of Tabriz, Marand Faculty of Engineering, Geomatics Engineering Department, Iran

Keywords
Remote sensing
Land surface temperature
Landsat
MODIS
LST validation

Abstract

Assessing the accuracy of the Land surface temperature (LST) has been and remains a challenging task. Rapid LST fluctuations in time and space, and a spatial scale mismatch between satellite and terrestrial sensors, have made validation using terrestrial data challenging. In addition to using ground data, there are three techniques for evaluating this parameter: radiance-based validation, indirect assessment, and cross-validation between two sensors. One of the most prevalent approaches for measuring LST accuracy is cross-validation. The main requirements of the cross-validation approach are temporal, spectral, spatial, and sensor angle of view adaptation. A technique for cross-validating LST from Landsat 8 using MODIS sensors is provided in this research. MODIS ' temperature product was chosen as the reference since it was collected twice per day by each of their sensors. The suggested method's results revealed that the accuracy evaluation in regions with high homogeneity, using the parameters of mean differences and root mean square error, has an accuracy of 0.6 and 1.63 degrees Kelvin in the first study's image, respectively. These values, 0.94 and 1.27 kelvin, were likewise achieved in the image of the second research. The suggested approach is applicable to any thermal sensor at any time and place.

1. Introduction

Surface temperature is one of the variables required in a wide range of earth science and environmental studies and research, as well as in numerous applications such as evapotranspiration modeling, soil moisture estimation, urban climate, hydrology, vegetation monitoring, and environmental studies. Remote sensing technology allows for large-scale geographical and temporal monitoring of this quantity. However, evaluating the accuracy and validation of this quantity has been and continues to be a difficult issue because, on the one hand, its rapid changes in the range of space and time, such as changing more than ten degrees Kelvin in a very short distance or more than one degree Kelvin in a very long time, have been and continue to be a challenge. It is brief (less than a minute)) Li et al., 2013; Prata, Caselles, Coll, Sobrino, & Ottle, 1995(but due to the incompatibility of the spatial scale between satellite and terrestrial sensors, its confirmation using terrestrial data is complex and challenging.

Although various methods for retrieving surface temperature from thermal data have been established in recent decades, validation of the temperature acquired from this data has not been developed due to the following issues, which need the creation of new algorithms))Coll et al., 2005; Guillevic et al., 2012; Pinker, Sun, Hung, Li, & Basara, 2009; Wan, 2008(. The primary issue with surface temperature validation is that ground-based temperature observations at the local scale have coupled impacts with ambient and atmospheric factors. Measuring the environment, which takes time and is tough to monitor. The second issue is measuring the surface temperature on a pixel scale using the terrestrial method, because each pixel image covers an area of a few hundred meters or kilometers due to spatial variation in surface characteristics and large spatiotemporal variations in the surface temperature itself. It's tough to think of a method for acquiring a reference temperature on a pixel scale. The third issue is temporal sampling of the surface temperature, which must be done at a very high frequency since the surface temperature might vary by several degrees owing to wind, shadow, and other environmental conditions. A three-step strategy for cross-validating ground surface temperature collected from Landsat 8 sensors with MODIS temperature sensor

* **Corresponding Author**

*(h_emami@ut.ac.ir) ORCID ID 0000-0002-0171-6487
(arahmanizadeh@tabrizu.ac.ir) ORCID ID xxxx – xxxx – xxxx – xxxx

Cite this study

Emami, H., & Rahmanizadeh, A. (2022). Introducing a new approach to temperature validation of remote sensing thermal images. 4th Intercontinental Geoinformation Days (IGD), 9-12, Tabriz, Iran

products in Fars provincial areas is provided in this research. MODIS' temperature product was chosen as a reference in cloud-free weather circumstances due to its vast coverage and collection twice per day by each of its sensors. Because our nation lacks a temperature validation database, our suggested technique relied on MODIS data only in homogenous thermal zones as a reference. As a result, the suggested approach may be used for any time-place and any thermal sensor.

2. Method

The steps in the proposed method are as follows: The study datasets were preprocessed and topographic and atmospheric correction were applied in the first step. In the second stage, the emission coefficients of different classes were calculated using the method of calculating surface emissivity, using the ASTER spectral library, Kirchhoff law, and the spectral response functions of Landsat 8 thermal bands. After producing the product temperature of the MODIS, Terra, and Aqua sensors, the appropriate processing was conducted on them, and the data was prepared to apply the suggested approach in the third step. The suggested approach is executed in three phases for temporal-spectral and spatial adaptation of the product of Landsat 8 and MODIS sensors in the fourth stage, and the results are studied and reviewed.

2.1. Study area and datasets

The research area is an arid and semi-arid region with a diversified land cover that includes heterogeneous pixels covered by various flora, soil, and rocky kinds. It is located between the latitudes of 26° 25'–32° 44'N and the longitudes of 50° 32'–55° 54'E. Figure 1 depicts the land use/land cover data recorded in June 2018, which included seventeen classes and two scenes of LDCM data.

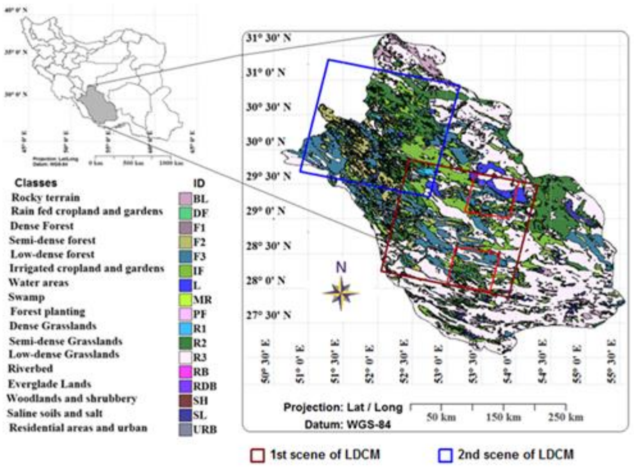

Figure 1. The study area with the seventeen-class land cover map

Besides the LDCM data, the LST products of MOD/MYD 11 L2 and MOD/MYD11A1 MODIS are employed in the current work for LST cross-comparison in the suggested scaling approach that is obtained from a generalized split-window algorithm.

2.2. The LST Retrieval

Having LSEs, to evaluate the impact of the LSE improvement on LST, based on the USGS recommendation on the LDCM data, the single channel (SC) algorithm of (Jiménez-Muñoz & Sobrino, 2003) is used. SC algorithm is utilized for sensitivity analysis using only band 10. Therefore, the σ_{alg} is below 1 K since the VW contents of the study area are 0.8 and 1.2 for examined datasets (Table I). The $SC^{JM\&S}$ algorithm retrieves LST (T_s) using the general (1).

$$T_s = \left(\left\{ \frac{k_2\, L_{sen}}{T_{sen}^2} \left[\frac{\lambda_e^4}{k_1} + \lambda_e^{-1} \right] \right\}^{-1} \right) * \left[\frac{1}{\varepsilon} \left(\psi_1\, L_{sen} + \psi_2 \right) + \psi_3 \right] + T_{sen} - \gamma L_{sen} \quad (1)$$

where L_{sen} is the at-sensor radiance in w m^2 sr^{-1} µm^{-1}, T_{sen} is the at-sensor brightness temperature in K, λ_e is the effective wavelength in µm, k_1 and k_2 are constant of thermal bands in W m^2 sr^{-1} µm^{-1} and K, respectively. ε is the surface emissivity and unitless, ψ_1, ψ_2, and ψ_3 are referred to as atmospheric functions (AFs) which computed by (2) (Jimenez-Munoz, Sobrino, Skokovic, Mattar, & Cristobal, 2014).

$$\psi_1 = \frac{1}{\tau}\ , \quad \psi_2 = -L^{\downarrow} - \frac{L^{\uparrow}}{\tau}\ , \quad \psi_3 = L^{\downarrow} \quad (2)$$

Where $L^{\uparrow}$ is the upwelling radiation and $L^{\downarrow}$ is the downwelling radiation in w m^2 sr^{-1} µm^{-1} and τ is unitless and atmospheric transmittance.

Table 1. Atmospheric parameters for band 10 LDCM

Scene ID	τ	$L^{\uparrow}$	$L^{\downarrow}$	$wv[gcm]^{-2}$
162-40	0.85	1.19	1.98	1.20
163-39	0.92	0.64	1.09	0.80

For each image, τ, $L^{\uparrow}$ and $L^{\downarrow}$ were obtained using online radiative transfer codes (http://www.atmcorr.gsfc.nasa.gov/) from Atmospheric Correction Parameter Calculator (ACPC)developed by NASA for Landsat satellites(J. Barsi, Barker, & Schott, 2003; J. A. Barsi, Schott, Palluconi, & Hook, 2005).

2.3. The LST Validation

Because there is no available database of *in situ* LST measurements that coincides with the LDCM satellite overpasses, is one of the major problems in LST validation in our case study. Generally, the LST changes rapidly in space and time, and it changes more than 10 K in a very short distance or more than 1 K in a very short time (less than one minute) (Li et al., 2013; Prata et al., 1995). Hence, the strong spatial heterogeneity and temporal variation of LST limit ground-based validation only to several relatively homogeneous surfaces (Tang & Li, 2014). Furthermore, the selection of homogeneous surface is scarce and a risky question. For this purpose, (Liu, Hiyama, & Yamaguchi, 2006) suggested that scaling methods must be developed to assist for the validation retrieved of LSTs. Since the acquisition date of the ASTER

LST product is asynchronous with the LDCM data, it is not possible to use it for LST cross-comparison. Therefore, due to the limited accessibility to the actual LSTs measured in situ, the daily LST products of MODIS (MOD/ MYD 11_L2 and MOD/MYD11A1 (V5)) were selected as the reference data. These products include 1 km pixels, using the SW algorithm. Because of the wide coverage and taken LST product twice per day by each of Terra and Aqua satellites, these products were selected as the reference temperature. The LST products of MODIS sensors have been validated with in situ measurements and by various methods in more than 50 clear-sky cases taking into account the higher accuracies less than 1°K for both Terra and Aqua (Qian, Li, & Nerry, 2013). In this regard, geographic coordinate matching, time matching and view zenith angle matching between LST of the LDCM data and the MODIS product arises for cross-comparison. To deal with these problems, we proposed an alternative scaling method of cross-comparison based on LST products of MODIS to yield a compatible dataset for accuracy assessment as in the following three steps.

In the first step, to consider the spatial resolution differences between the LDCM and MODIS LST products, the obtained LST of LDCM data by the proposed and compared methods should be scaled up to the MODIS LST product with 1km spatial resolution. Hence, similar to (Qian et al., 2013) which provided the aggregation algorithm area-weighted pixel, the LST of LDCM data aggregated to the same spatial resolution of the MODIS product using an 11 x 11 processing window size. After scale up between the two sensors, it certainly cannot be said that the pixels in terms of spectral range are the same. Because spectral data received by the sensor depends on several factors such as the surface emissivity, surface topography, zenith angle of sensor, misregistration error between the sensors data and so on. Therefore, in the second step, for spectral and view zenith angle matching, the thermal homogeneity area was determined. The select thermal homogeneous regions not only confirm time-invariant assumption of LSE (Tang & Li, 2014) but also the impact of misregistration on LSE and LST between different sensor data, makes little and negligible (Wan, 1999). That is, co-occurrence matrix (CM) which contains a large amount of local spatial information about an image is used. A set of texture features derived from the CM matrix was suggested by (Haralick, Shanmugam, & Dinstein, 1973). In particular, two texture features of the inverse difference moment (IDM) and angular second moment (ASM) describe the homogeneity in an image.

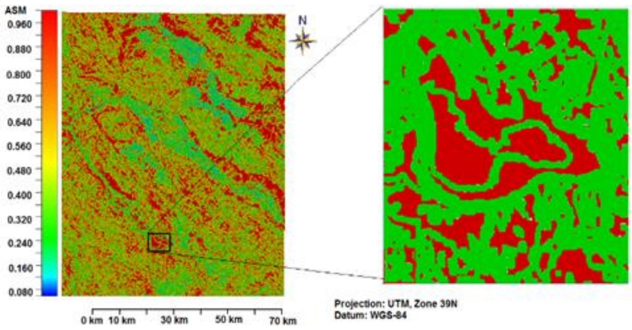

Figure 2. Example of extracted homogeneous regions

An 11 x 11 processing window size was selected and homogeneity measures were obtained. The processing window size is selected as spatial resolution of MODIS is about ten times of LDCM thermal bands. Fig.2 shows an example of extracted homogeneity regions on ASM feature. In this research, the areas with homogeneity content between 0.9 and 1 were selected as testing and validation sites in both homogeneity features.

The third step is time matching between LST of the LDCM data and MODIS products. In this regard, the approximate overpass times of the Terra and Aqua satellites in study area (scan start times from 01:30 to 24:00 UTC for MOD/ MYD 11_L2 and MOD/MYD 11 A1products) were considered during a day. Then coordinates matching between LST MODIS products are performed. Afterward, for each selected validation point at least five overpass times of LST MODIS products are selected. In weather condition that is sunny and cloud free, the main factor controlling the surface temperature is radiation and energy of sun. Usually, solar radiation changes during a day is almost a sine function. It is worthy to note that the situation in study area is same as aforementioned weather condition. Accordingly, we modeled the pattern of surface temperature changes during the day, as a sinusoidal function at a given point as (3).

$$LST_{ij}^{Modis} = a_i + b_i \times \cos\left(c_i T_{ij}^{Modis} + d_i \right) \qquad (3)$$

Where LST_{ij}^{MODIS} is the LST of the i*th* point at the j*th* overpass time, T_{ij}^{MODIS} is the j*th* overpass time of Terra or Aqua over the i*th* point and a_i, b_i, c_i, and d_i are constant coefficients of the i*th* point. For the i*th* point, these coefficients were obtained by five available LSTs of MODIS. Accuracy of (13) that obtained for each validation point is less than one degree Kelvin that is the range of accuracy of MODIS LST product. Fig.16 shows a sample of the sinusoidal function obtained for a desired point. Finally, the LST of MODIS is yielded at the overpass time of LDCM for the i*th* point by (3) as reference values for LST validation. It is worth noting that the proposed sinusoidal function in (3) can only describe the LST variation for entire clear days with at least five LST values in during a day.

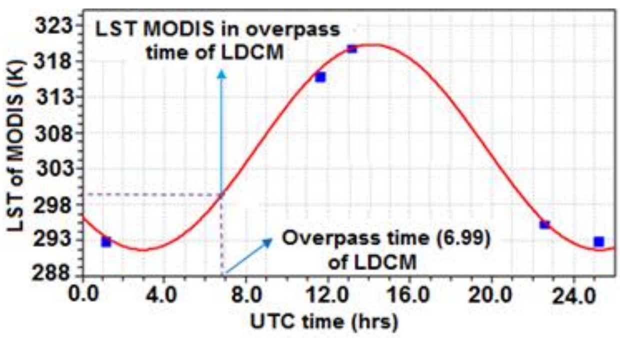

Figure. 3. The model of daily temperature change obtained by LST of MODIS products.

3. Results

To validate the suggested approach, two Landsat 8 images were selected at separate times, and 38 and 62 validation points in high homogeneity regions (0.90 to 1.0) were recovered from the first and second images, respectively. In the first and second Landsat 8 images, homogeneity (0.80 to 0.90) was calculated using 30 and 49 points, respectively. The outcomes evaluation is described below.

Table 2. Surface temperature comparison between Landsat 8 and MODIS products during Landsat 8 transit duration at validation locations.

LST_{LDCM}- $LST^{opt.Ldcm}_{MODIS}$				
SD_{ST}(K)	RMSE(K)	N	homogeneity	Image ID
1.79	1.72	38	0.90-1.00	162-40
1.73	1.95	62	0.90-1.00	163-39
4.96	4.82	30	0.80-0.90	162-40
3.79	4.58	49	0.80-0.90	163-39

4. Conclusion

In this paper, an alternative scaling method based on LST products of MODIS was proposed for LST cross-comparison. According to the findings of this study, validation points should come from regions with high homogeneity for many applications at the local scale, such as evapotranspiration modeling, soil moisture estimation, urban climate, hydrology, vegetation monitoring, and environmental studies. In the illustration, (0.90 to 1.00) is chosen. Such environments include heavily vegetated areas, aquatic areas such as dams or lakes, salt marshes, and similar thermally homogeneous places where vegetation and aquatic areas may be seen in most photos. In this proposed technique, thermal homogenous regions were employed to assess and validate the surface temperature. Areas with homogeneity in the range (0.80 to 1.00) can also be selected and utilized for global-scale applications that need less precision in computing the surface temperature of validation sites. In general, the benefit of employing the suggested approach is that no ground temperature observations are required. Furthermore, this approach, in addition to being a robust method for measuring the accuracy of surface temperature, is applicable for any time and location, as well as any thermal sensor, due to the lack of a temperature validation database in our nation.

References

Barsi, J., Barker, J. L., & Schott, J. R. (2003). *An atmospheric correction parameter calculator for a single thermal band earth-sensing instrument.* Paper presented at the IEEE International Geoscience and Remote Sensing Symposium, 2003. IGARSS'03. Proceedings.

Barsi, J. A., Schott, J. R., Palluconi, F. D., & Hook, S. J. (2005). *Validation of a web-based atmospheric correction tool for single thermal band instruments.* Paper presented at the Optics & Photonics 2005.

Coll, C., Caselles, V., Galve, J. M., Valor, E., Niclos, R., Sánchez, J. M., & Rivas, R. (2005). Ground measurements for the validation of land surface temperatures derived from AATSR and MODIS data. *Remote Sensing of Environment, 97*(3), 288-300.

Guillevic, P. C., Privette, J. L., Coudert, B., Palecki, M. A., Demarty, J., Ottlé, C., & Augustine, J. A. (2012). Land Surface Temperature product validation using NOAA's surface climate observation networks—Scaling methodology for the Visible Infrared Imager Radiometer Suite (VIIRS). *Remote Sensing of Environment, 124*, 282-298.

Haralick, R. M., Shanmugam, K., & Dinstein, I. H. (1973). Textural features for image classification. *IEEE Transactions on Systems, Man and Cybernetics, 3*(6), 610-621.

Jimenez-Munoz, J. C., Sobrino, J., Skokovic, D., Mattar, C., & Cristobal, J. (2014). Land surface temperature retrieval methods from Landsat-8 thermal infrared sensor data. *Geoscience and Remote Sensing Letters, IEEE, 11*(10), 1840-1843.

Jiménez-Muñoz, J. C., & Sobrino, J. A. (2003). A generalized single-channel method for retrieving land surface temperature from remote sensing data. *Journal of Geophysical Research: Atmospheres (1984–2012), 108*(D22).

Li, Z.-L., Tang, B.-H., Wu, H., Ren, H., Yan, G., Wan, Z., . . . Sobrino, J. A. (2013). Satellite-derived land surface temperature: Current status and perspectives. *Remote Sensing of Environment, 131*, 14-37.

Liu, Y., Hiyama, T., & Yamaguchi, Y. (2006). Scaling of land surface temperature using satellite data: A case examination on ASTER and MODIS products over a heterogeneous terrain area. *Remote Sensing of Environment, 105*(2), 115-128.

Pinker, R. T., Sun, D., Hung, M.-P., Li, C., & Basara, J. B. (2009). Evaluation of satellite estimates of land surface temperature from GOES over the United States. *Journal of Applied Meteorology and Climatology, 48*(1), 167-180.

Prata, A., Caselles, V., Coll, C., Sobrino, J., & Ottle, C. (1995). Thermal remote sensing of land surface temperature from satellites: Current status and future prospects. *Remote Sensing Reviews, 12*(3-4), 175-224.

Qian, Y.-G., Li, Z.-L., & Nerry, F. (2013). Evaluation of land surface temperature and emissivities retrieved from MSG/SEVIRI data with MODIS land surface temperature and emissivity products. *International Journal of Remote Sensing, 34*(9-10), 3140-3152.

Tang, H., & Li, Z.-L. (2014). Quantitative Remote Sensing in Thermal Infrared: Theory and Applications (pp. 257-279): Springer Berlin Heidelberg.

Wan, Z. (1999). MODIS land-surface temperature algorithm theoretical basis document (LST ATBD). *Institute for Computational Earth System Science, Santa Barbara, 75*.

Wan, Z. (2008). New refinements and validation of the MODIS land-surface temperature/emissivity products. *Remote Sensing of Environment, 112*(1), 59-74.